



## Multiple nodeless superconducting gaps in optimally doped SrTi<sub>1-x</sub>Nb<sub>x</sub>O<sub>3</sub>

Xiao Lin,<sup>1</sup> Adrien Gourgout,<sup>1,2</sup> German Bridoux,<sup>1,\*</sup> François Jomard,<sup>3</sup> Alexandre Pourret,<sup>2</sup> Benoît Fauqué,<sup>1</sup> Dai Aoki,<sup>2,4</sup> and Kamran Behnia<sup>1,†</sup>

<sup>1</sup>Laboratoire Physique et Etude de Matériaux–CNRS/ESPCI/UPMC, F-75005 Paris, France

<sup>2</sup>Institut Nanosciences et Cryogénie, SPSMS, CEA/UJF, F-38054 Grenoble, France

<sup>3</sup>Groupe d'Étude de la Matière Condensée, F-78035 Versailles, France

<sup>4</sup>Institute for Materials Research, Tohoku University, Oarai, Ibaraki 311-1313, Japan

(Received 8 September 2014; published 29 October 2014)

We present a study of thermal conductivity in superconducting SrTi<sub>1-x</sub>Nb<sub>x</sub>O<sub>3</sub>, sufficiently doped to be near its maximum critical temperature. The bulk critical temperature, determined by the jump in specific heat, occurs at a significantly lower temperature than the resistive  $T_c$ . Thermal conductivity, dominated by the electron contribution, deviates from its normal-state magnitude at bulk  $T_c$ , following a Bardeen-Rickayzen-Tewordt behavior, which is expected for thermal transport by Bogoliubov excitations. The absence of a  $T$ -linear term at very low temperatures rules out the presence of nodal quasiparticles. On the other hand, the field dependence of thermal conductivity points to the existence of at least two distinct superconducting gaps. We conclude that optimally doped strontium titanate is a multigap nodeless superconductor.

DOI: [10.1103/PhysRevB.90.140508](https://doi.org/10.1103/PhysRevB.90.140508)

PACS number(s): 74.25.fc, 74.20.Fg, 74.20.Rp, 74.62.Dh

Discovered as early as 1964 [1], the superconducting state of  $n$ -doped SrTiO<sub>3</sub> (STO) occupies a singular place in the history of superconductivity. Besides being the first oxide superconductor, it was one of the earliest “semiconducting superconductors” [2], the first experimentally detected multigap superconductor [3], and the first case of a superconducting dome [4]. Half a century after its discovery, it remains the most dilute superconductor, with its Cooper pairs springing out of the tiniest Fermi surface known to undergo such a transition [5].

In spite of this importance, and the intense attention devoted to the two-dimensional superconductivity discovered in SrTiO<sub>3</sub> heterojunctions [6], the symmetry of the superconducting order parameter of this system has remained a virgin field of exploration. Besides the early report on two distinct superconducting gaps detected by planar tunneling experiments [3], little is known about the superconducting gap and its structure. In the absence of experimental data coming from bulk probes, the existence of nodes in the superconducting gap remains an open question. Moreover, in contrast to early tunneling experiments, a recent study on superconducting interfaces did not detect multiple superconducting gaps [7].

A phase transition to a superconducting ground state modifies the electronic component of heat transport. Mobile electrons are replaced by Cooper pairs and Bogoliubov quasiparticles. Only the latter carry heat and they vanish in the zero-temperature limit. Therefore, any residual electronic contribution to thermal conductivity in this limit, often detected as a  $T$ -linear term, can be safely attributed to the presence of nodal quasiparticles of a sign-changing gap. In the past two decades, thermal conductivity has emerged as a sensitive probe of such nodal quasiparticles [8]. It has been used to detect both nodal and nodeless gaps of a variety of unconventional superconductors. The list includes heavy-fermion [9,10],

cuprate [11–14], ruthenate [15], organic [16,17], and iron-based [18,19] superconductors. Thermal conductivity has also been used to establish the multiplicity of superconducting gaps. Beyond the emblematic case of MgB<sub>2</sub> [20], several other extensively studied superconductors, including NbSe<sub>2</sub> [21] and CeCoIn<sub>5</sub> [22,23], were identified as multiband superconductors owing to thermal conductivity measurements. In this Rapid Communication, we present a study of thermal conductivity in optimally doped strontium titanate and find unambiguous evidence for the absence of nodal quasiparticles and for the multiplicity of superconducting gaps. This paves the way for the identification of the symmetry of the superconducting order parameter and the determination of the relative weight of interband and intraband pairing strength [24].

The SrTiO<sub>3</sub>:Nb single crystals used in this study were commercial substrates such as those used in previous studies on metal-insulator transitions [25] and fermiology [5,26] in  $n$ -doped SrTiO<sub>3</sub>. Figure 1(a) presents the doping dependence of the resistive superconducting transition in these samples. The carrier concentration was determined by measuring the Hall coefficient and was found to be in good agreement with the expected value according to the nominal Nb content. The latter was directly checked by secondary ion beam mass spectroscopy (SIMS) (see the Supplemental Material [27]).

The sample chosen for an extended study has a resistive critical temperature as high as 0.44 K [Fig. 1(a)]. Owing to its relatively high carrier concentration, it has a predominant electronic contribution to its specific heat and thermal conductivity. This sample was cut into two pieces. One was used for a study of heat capacity and the other for transport. Thermal conductivity, concomitant with electrical resistivity, was measured by a standard one-heater–two-thermometers setup. Measurements were also carried out on three other samples with different carrier concentrations and led to similar results (see the Supplemental Material). The focus here will be on the extended set of data obtained on one particular sample.

Figure 1(b) presents the jump in specific heat caused by the superconducting transition. An early measurement, limited downward to 0.3 K, detected the beginning of an upturn in

\*Present address: Consejo Nacional de Investigaciones Científicas y Técnicas, CONICET, Tucuman, 4000, Argentina.

†kamran.behnia@espci.fr

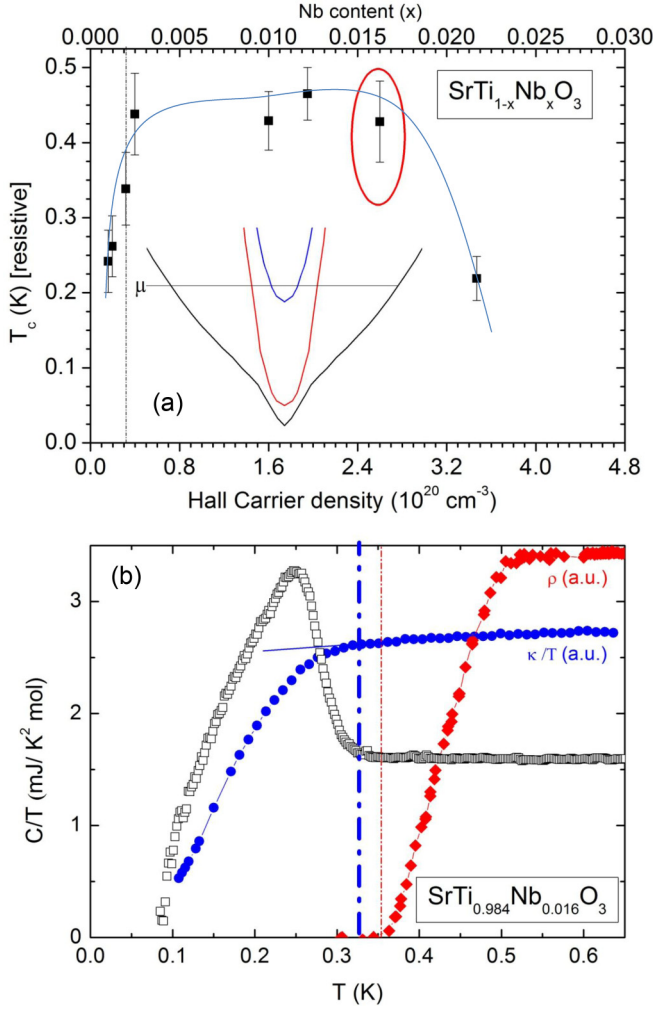


FIG. 1. (Color online) (a) Variation of resistive critical transition in Nb-doped SrTiO<sub>3</sub> with carrier concentration (determined by the Hall coefficient). Above the critical doping, marked by a vertical line, three bands are occupied, as sketched in the inset. The symbol representing the sample subject to the in-depth study in this work is surrounded by a red ellipse. (b) The temperature dependence of heat capacity divided by temperature (open squares), compared with thermal conductivity divided by temperature (solid circles) and electrical resistivity (solid diamonds). The dotted-dashed vertical lines mark the end of the resistive and the beginning of the bulk superconducting transitions.

specific heat [28]. Our observation definitely confirms that this is a phase transition of bulk electrons. Two other pieces of information can be extracted from the specific heat data. The first is the onset temperature of bulk superconductivity. As seen in the figure, the jump starts at 0.33 K, which is significantly lower than the temperature at which resistivity vanishes ( $\sim 0.35$  K). Second, the magnitude of the  $T$ -linear electronic specific heat in the normal state ( $\gamma \simeq 1.55$  mJ mol<sup>-1</sup> K<sup>-2</sup>) is remarkably large for a dilute metal with a carrier concentration of  $n_H = 2.6 \times 10^{20}$  cm<sup>-3</sup>. Copper, with a carrier density 300 times larger, has a  $\gamma$  that is twice lower. The large  $\gamma$  is a consequence of significant mass enhancement in doped SrTiO<sub>3</sub>. If all electrons were in a single spherical Fermi surface, using the expression  $\gamma = \frac{m^* k_F}{3} \left(\frac{k_B}{\hbar}\right)^2$ , one would

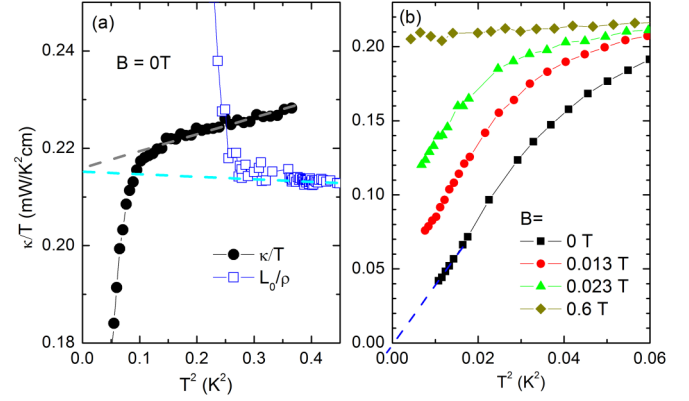


FIG. 2. (Color online) (a) In agreement with the Wiedemann-Franz law, the thermal conductivity divided by temperature  $\kappa/T$  (solid circles) and the Lorenz number divided by resistivity  $L_0/\rho$  (solid squares) of the normal state ( $T > T_c$ ) extrapolate both to the same value. (b)  $\kappa/T$  as a function of  $T^2$  for different magnetic fields. At zero magnetic field, extrapolating  $\kappa/T$  to zero temperature leads to a vanishing intercept.

find an effective mass of  $m^* = 4.2m_e$ . This agrees with the conclusions of the study of quantum oscillations, according to which, when the carrier concentration exceeds  $2 \times 10^{19}$  cm<sup>-3</sup>, three bands are occupied, with most carriers residing in the lowest and heaviest band with an effective mass as large as  $4m_e$  [26]. Thus, two distinct experimental probes converge in finding an effective mass that is twice as large as the band mass [29].

The thermal conductivity data are also shown in Fig. 1(b). As seen in the figure,  $\kappa/T$  does not show any detectable feature at resistive  $T_c$ , but starts to deviate from its normal-state value as soon as the jump in specific heat starts. The bulk phase transition begins at a temperature which is 20 mK lower than the end of the resistive transition. We will come back to this feature below.

The first experimental check on the accuracy of our thermal conductivity data is the verification of the Wiedemann-Franz (WF) law. As seen in Fig. 2(a), the normal-state thermal conductivity extrapolates to slightly below  $0.22$  mW K<sup>-2</sup> cm<sup>-1</sup> at zero temperature. Given the residual resistivity of the sample ( $110 \mu\Omega$  cm), one finds a Lorenz number close to the expected  $L_0 = 2.44 \times 10^{-8}$  V<sup>2</sup> K<sup>-2</sup>. As seen in the figure, at the onset of the resistive superconducting transition,  $\frac{L_0}{\rho}$  is nine-tenths of  $\kappa/T$ , implying an electron contribution roughly ten times the lattice component of heat transport. This simplifies the analysis and strengthens the conclusion.

Figure 2(b) presents the temperature dependence of thermal conductivity at different magnetic fields. At 0.6 T, superconductivity is destroyed and thermal conductivity yields a large linear term, very close to the zero-field value and the expected WF value. In the absence of magnetic field, in the superconducting state, thermal conductivity rapidly decreases with decreasing temperature. As seen in the figure, in this case, a linear extrapolation of  $\kappa/T$  vs  $T^2$  to  $T = 0$  has no detectable intercept. This result, reproduced on other samples with different carrier concentrations and mobilities (see the Supplemental Material), is the first main result of this work.

In the presence of nodal quasiparticles, one would expect a residual  $T$ -linear term in thermal conduction, on top of the phononic  $T^3$  term [11]. This is clearly not our case.

The  $T^3$  term of thermal conductivity sets an upper limit to the phonon conductivity. Using the kinetic formula  $\kappa_{\text{ph}} = 1/3 C_{\text{ph}} v_s \ell_{\text{ph}}$  and the reported values for lattice heat capacity ( $C_{\text{ph}} = \beta T^3$ ;  $\beta = 0.58 \text{ J K}^{-4} \text{ m}^{-3}$  [28]) and average sound velocity ( $\langle v_{\text{ph}} \rangle = 5300 \text{ ms}^{-1}$  [30]), one can estimate the upper limit to the phonon mean free path of phonons. If  $\kappa_{\text{ph}} = bT^3$  with  $b = 3.8 \text{ mW K}^{-4} \text{ cm}^{-1}$ , one obtains a phonon mean free path of 0.35 mm, to be compared with a sample thickness of 1 mm. Thus, even at temperatures as low as 0.1 K, and in the absence of scattering by electrons, phonon transport may not be fully ballistic. We note that the structural transition at 105 K, in the absence of strain, would create three equivalent tetragonal domains in a SrTiO<sub>3</sub> single crystal. The domain boundaries, which are macroscopically long [31], may play a role in setting the ultimate low-temperature mean free path of phonons.

In presence of  $B = 0.6 \text{ T}$ , when the normal state survives down to the lowest temperature, one can use the Wiedemann-Franz to separate the electronic,  $\kappa_e^N$ , and lattice,  $\kappa_{\text{ph}}^N$ , components of thermal conductivity. In the superconducting state, on the other hand, one cannot separate  $\kappa_e^S$  and  $\kappa_{\text{ph}}^S$  in a straightforward fashion. By vanishing in to the superconducting condensate, electrons open the road for an enhanced lattice conductivity of unknown magnitude. An upper bound to the lattice conductivity is given by the magnitude of the asymptotic  $T^3$  thermal conductivity. By assuming that the phonon mean free path linearly increases from  $T_c$  to its maximum value at 0.1 K, with  $\kappa_{\text{ph}}^S$  accounting for half of the total thermal conductivity, we found a  $\kappa_e^S(T)$  in excellent agreement with the Bardeen, Rickayzen, and Tewordt (BRT) function with plausible parameters (a  $T_c$  of 0.33 K and a gap of 0.74 K). This function is the cornerstone of the standard theory of heat transport in a conventional superconductor [32]. The decomposition of thermal conductivity to its lattice and electronic components, as well as the fit to the BRT function, are shown in the two panels of Fig. 3. Given the arbitrary assumption on  $\kappa_{\text{ph}}^S(T)$  mentioned above, this should only be taken as a qualitative sketch. A  $T_c$  of 0.33 K is in excellent agreement with the heat capacity data and a gap of 0.74 K ( $=64 \text{ } \mu\text{eV}$ ) is close to what was seen by tunneling measurements close to this doping range (60–80  $\mu\text{eV}$ ) [3]. Note, however, that these would yield a  $\frac{\Delta}{k_B T_c}$  ratio of 2.2, compared to the BCS value of 1.76.

Up to here, no feature of heat transport distinguishes this superconductor from aluminum, in which the BRT function was experimentally checked decades ago [33]. As soon as one examines the effect of magnetic field, however, such a distinction becomes visible. As seen in Fig. 4, the application of a small magnetic field, which is much lower than the upper critical field  $H_{c2}$ , substantially modifies the magnitude of thermal conductivity. Moreover, by sweeping the magnetic field from zero to  $H_{c2}$ , a shoulder is detectable in  $\kappa(H)$ . Both these features were detected in multiband superconductors [8,20–23] and were interpreted as the signatures of multigap superconductivity.

In a nodeless single-band superconductor, the application of magnetic field, as far as the distance between the vortices

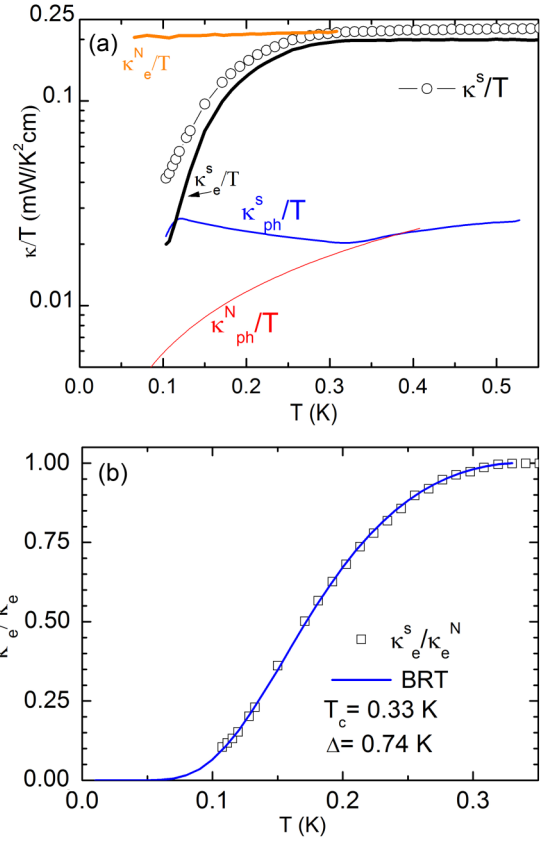


FIG. 3. (Color online) (a) Zero-field thermal conductivity of the superconducting state (open circles) as a function of temperature. Electronic and lattice components of thermal conductivity in normal ( $B = 0.6 \text{ T}$ ) and superconducting ( $B = 0$ ) states are shown as solid lines. In the normal state, the Wiedemann-Franz law allows an unambiguous determination of  $\kappa_{\text{ph}}^N$  and  $\kappa_e^N$ . In the superconducting state,  $\kappa_{\text{ph}}^S$  and  $\kappa_e^S$  were estimated by assuming that the phonon mean free path at  $T_c$  linearly increases to a saturated maximum of  $150 \text{ } \mu\text{m}$  at  $T = 0.1 \text{ K}$ . (b) The best fit of  $\kappa_e^S$  to a BRT function yielding the gap and the  $T_c$  as parameters.

keeps the quasiparticles trapped inside the normal cores of the vortices, does not affect heat transport. On the other hand, in a multiband superconductor, a modest magnetic field can significantly enhance thermal conductivity by closing the smaller gap. As seen in the lower inset of Fig. 4(a), which compares our case with three other superconductors, this is the case of Nb-doped SrTiO<sub>3</sub>.

Thermal conductivity becomes independent of magnetic field above a threshold magnetic field, which is 0.08 T at 0.097 K [see the upper inset of Fig. 4(a)]. This field is the bulk upper critical field  $H_{c2}^{\text{bulk}}$ . Below a second field scale  $H^*$  that is lower than  $H_{c2}^{\text{bulk}}$ , thermal conductivity shows a steeper field dependence. This second field scale points to the existence of an additional superconducting coherence length. In a multiband system, there can be several distinct length scales with their amplitude set by the linear combinations of gaps in different bands [34].

We did not detect a third scale of magnetic field in this three-band system. In this respect, our results are similar to those reported by Binnig *et al.* [3], who detected two (and

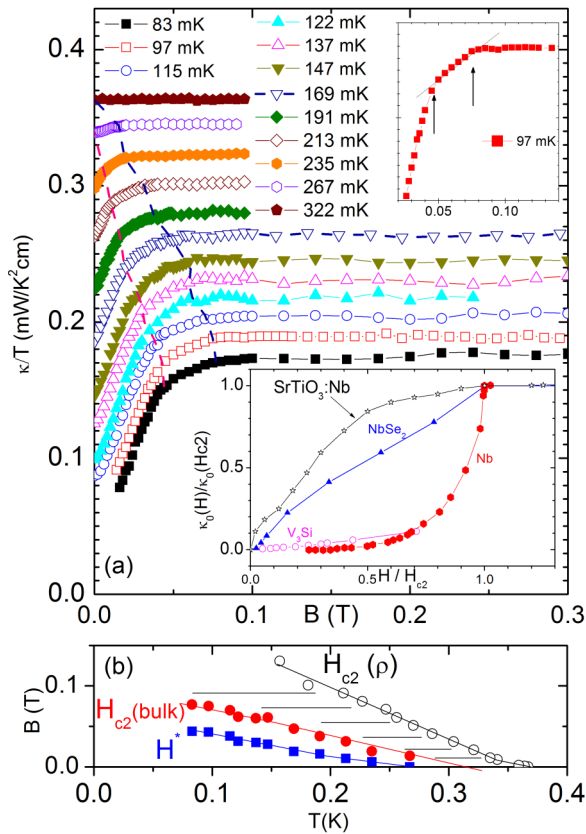


FIG. 4. (Color online) (a) The field dependence of thermal conductivity at different temperatures reveals a shoulder at a field  $H^*$  below  $H_{c2}$ . This is more clearly seen in the upper inset. The lower inset compares the field dependence of thermal conductivity in Nb-doped  $\text{SrTiO}_3$ , a multigap ( $\text{NbSe}_2$ ) and two single-gap ( $\text{Nb}$  and  $\text{V}_3\text{Si}$ ) superconductors (see Refs. [8,21]). (b) The two field scales extracted from  $\kappa(H)$  compared to  $H_{c2}(\rho)$ , the magnetic field at which resistivity vanishes. In the region filled with horizontal lines the resistivity vanishes, but bulk electrons are still normal.

not three) distinct superconducting gaps. Two possibilities come to mind. Either two of the bands have gaps of almost identical magnitudes, or the one associated with the third band (and the corresponding field scale) is too small to be easily detectable. The initial rise of thermal conductivity by a small

magnetic field, which is much lower than  $H^*$ , is either due to the existence of a third field scale that is much smaller than the other two, or a strong anisotropy of one of the two detected gaps. Note, however, that in the presence of interband coupling there is a nontrivial relationship between the length scales and the amplitudes of the gap.

As seen in Fig. 4(b), the bulk upper critical field is significantly lower than the resistive upper critical field. The result is confirmed by specific heat data in the presence of magnetic field (see the Supplemental Material). This brings us back to the shift observed at zero magnetic field between the bulk transition temperature and vanishing resistivity. In a portion of the  $(B, T)$  plane, bulk electrons are still normal, but the system shows zero resistivity. This calls for an explanation. Invoking sample inhomogeneity does not provide an answer. In a wide doping range, the critical temperature does not show a strong dependence on doping. Moreover, the observation of quantum oscillations with a well-defined frequency corresponding to the density of bulk carriers estimated from the Hall effect puts an upper limit to any macroscopic inhomogeneity.

One place for superconductivity to survive when bulk electrons are normal are boundaries between tetragonal domains. If the critical temperature happens to be higher in these twin boundaries than in the bulk, one can observe a vanishing resistivity at a temperature well above the bulk critical temperature. Recent near-field studies on the STO interfaces have detected enhanced electrical conductivity along twin boundaries [35,36], providing plausibility to this speculation.

In summary, we find that optimally doped  $\text{SrTiO}_3:\text{Nb}$  is a multigap superconductor and none of its gaps has nodes. These are interesting pieces in this puzzle of exceptionally dilute superconductivity, for which several exotic pairing mechanisms (such as a phonon soft mode [37], plasmons [38], or ferroelectric quantum criticality [39]) have been proposed. In contrast to other known cases of multiband superconductivity, one can here tune the Fermi surface (in sheer size as well as the number of its components) across several orders of doping concentration. This provides different experimental opportunities and stronger constraints for theory.

We thank L. Taillefer for stimulating discussions. This work is supported by Agence Nationale de la Recherche as a part of QUANTHERM and SUPERFIELD projects.

- [1] J. F. Schooley, W. R. Hosler, and M. L. Cohen, *Phys. Rev. Lett.* **12**, 474 (1964).
- [2] J. K. Hulm, D. Ashkin, D. W. Deis, and C. K. Jones, *Prog. Low Temp. Phys.* **6**, 205 (1970).
- [3] G. Binnig, A. Baratoff, H. E. Hoening, and J. G. Bednorz, *Phys. Rev. Lett.* **45**, 1352 (1980).
- [4] J. F. Schooley, R. W. Hosler, E. Ambler, J. H. Becker, M. L. Cohen, and C. S. Koonce, *Phys. Rev. Lett.* **14**, 305 (1965).
- [5] X. Lin, Z. Zhu, B. Fauqué, and K. Behnia, *Phys. Rev. X* **3**, 021002 (2013).
- [6] N. Reyren *et al.*, *Science* **317**, 1196 (2007).
- [7] C. Richter *et al.*, *Nature (London)* **502**, 528 (2013).
- [8] For a review, see H. Shakeripour, C. Petrovic, and L. Taillefer, *New J. Phys.* **11**, 055065 (2009).
- [9] H. Suderow, J. P. Brison, A. Huxley, and J. Flouquet, *Phys. Rev. Lett.* **80**, 165 (1998).
- [10] Y. Machida, A. Itoh, Y. So, K. Izawa, Y. Haga, E. Yamamoto, N. Kimura, Y. Onuki, Y. Tsutsumi, and K. Machida, *Phys. Rev. Lett.* **108**, 157002 (2012).
- [11] L. Taillefer, B. Lussier, R. Gagnon, K. Behnia and H. Aubin, *Phys. Rev. Lett.* **79**, 483 (1997).
- [12] S. Nakamae, K. Behnia, L. Balicas, F. Rullier-Albenque, H. Berger, and T. Tamegai, *Phys. Rev. B* **63**, 184509 (2001).
- [13] C. Proust, E. Boaknin, R. W. Hill, L. Taillefer, and A. P. Mackenzie, *Phys. Rev. Lett.* **89**, 147003 (2002).

- [14] C. Proust, K. Behnia, R. Bel, D. Maude, and S. I. Vedenev, *Phys. Rev. B* **72**, 214511 (2005).
- [15] M. Suzuki, M. A. Tanatar, N. Kikugawa, Z. Q. Mao, Y. Maeno, and T. Ishiguro, *Phys. Rev. Lett.* **88**, 227004 (2002).
- [16] S. Belin and K. Behnia, *Phys. Rev. Lett.* **79**, 2125 (1997).
- [17] S. Belin, K. Behnia, and A. Deluzet, *Phys. Rev. Lett.* **81**, 4728 (1998).
- [18] M. A. Tanatar *et al.*, *Phys. Rev. B* **84**, 054507 (2011).
- [19] J.-Ph. Reid *et al.*, *Phys. Rev. Lett.* **109**, 087001 (2012).
- [20] A. V. Sologubenko, J. Jun, S. M. Kazakov, J. Karpinski, and H. R. Ott, *Phys. Rev. B* **66**, 014504 (2002).
- [21] E. Boaknin *et al.*, *Phys. Rev. Lett.* **90**, 117003 (2003).
- [22] M. A. Tanatar *et al.*, *Phys. Rev. Lett.* **95**, 067002 (2005).
- [23] G. Seyfarth, J. P. Brison, G. Knebel, D. Aoki, G. Lapertot, and J. Flouquet, *Phys. Rev. Lett.* **101**, 046401 (2008).
- [24] R. M. Fernandes, J. T. Haraldsen, P. Wölfle, and A. V. Balatsky, *Phys. Rev. B* **87**, 014510 (2013).
- [25] A. Spinelli *et al.*, *Phys. Rev. B* **81**, 155110 (2010).
- [26] X. Lin, G. Bridoux, A. Gourgout, G. Seyfarth, S. Krämer, M. Nardone, B. Fauqué, and K. Behnia, *Phys. Rev. Lett.* **112**, 207002 (2014).
- [27] See Supplemental Material at <http://link.aps.org/supplemental/10.1103/PhysRevB.90.140508> for details on niobium content, doping dependence of thermal conductivity and specific heat in presence of magnetic field.
- [28] E. Ambler, J. H. Colwell, W. R. Hosler, and J. F. Schooley, *Phys. Rev.* **148**, 280 (1966).
- [29] D. van der Marel, J. L. M. van Mechelen, and I. I. Mazin, *Phys. Rev. B* **84**, 205111 (2011).
- [30] W. Rewald, *Solid State Commun.* **8**, 607 (1970).
- [31] A. Buckley, J. P. Rivera, and E. K. H. Salje, *J. Appl. Phys.* **86**, 1653 (1999).
- [32] J. Bardeen, G. Rickayzen, and L. Tewordt, *Phys. Rev.* **113**, 982 (1959).
- [33] C. B. Satterthwaite, *Phys. Rev.* **125**, 873 (1962).
- [34] M. Silaev and E. Babaev, *Phys. Rev. B* **85**, 134514 (2012).
- [35] B. Kalisky *et al.*, *Nat. Mater.* **12**, 1091 (2013).
- [36] M. Honig, J. A. Sulpizio, J. Drori, A. Joshua, E. Zeldov, and S. Ilani, *Nat. Mater.* **12**, 1112 (2013).
- [37] J. Appel, *Phys. Rev.* **180**, 508 (1969).
- [38] Y. Takada, *J. Phys. Soc. Jpn.* **49**, 1267 (1980).
- [39] S. E. Rowley, L. J. Spalek, R. P. Smith, M. P. M. Dean, M. Itoh, J. F. Scott, G. G. Lonzarich, and S. S. Saxena, *Nat. Phys.* **10**, 367 (2014).